Altimeter-Derived Loop Current Metrics

Robert R. Leben

Colorado Center for Astrodynamics Research, University of Colorado, Boulder

Altimeter-derived Loop Current metrics are used to describe Loop Current intrusion and eddy separation in the Gulf of Mexico for the time period from 1 January 1993 through 1 July 2004. Time series of Loop Current extent, boundary length, area, circulation and volume are determined by tracking the 17-cm contour in the daily sea surface height maps. This contour closely tracks the edge of the high-velocity core of the Loop Current. The altimetric Loop Current tracking is qualitatively and quantitatively evaluated by direct comparisons with Loop Current thermal fronts observed in sea surface temperature imagery during times of good thermal contrast and cloud free conditions. Eddy separation events are identified by the changes in the Loop Current length associated with breaking of the tracking contour, with a total of 16 Loop Current eddies causing significant changes in the Loop Current extent during the time period. Statistical and spectral analyses are used to characterize the Loop Current variability and separation frequency. Eddy separation occurs most frequently at 6, 9 and 11.5 months, with little or no power at the annual frequency. Significant low frequency power is found near a period of 17 to 22 months, which is associated with far southern retreat of the Loop Current and separation periods near 18 months. A bimodal distribution of the retreat after eddy separation is identified that influences the duration of the subsequent separation period. When the entire Loop Current retreats below 25ºN the average separation period following retreat is 16.2 months, much longer than the 5.5 month average for the cases where part of the Loop Current remains north of 25ºN. More interesting is a nearly linear relationship between Loop Current retreat and subsequent separation periods. Thus the irregular retreat of the Loop Current after separation may explain in part why the Loop Current exhibits such an irregular eddy separation period.

1. INTRODUCTION

The Loop Current is the energetic section of the Gulf Stream System that "loops" in a clockwise direction within the Gulf of Mexico (GOM) after entering as a northward flowing current through the Yucatan Channel and later exiting to the east through the Florida Straits. The northward penetration of the Loop Current into the eastern GOM deep basin varies with time and at irregular intervals becomes great enough to produce large anticyclonic rings of recirculating current known as Loop Current eddies. Separation is defined as the final detachment of an eddy from the Loop Current with no later reattachment. Although eddies may frequently detach from and reattach to the Loop Current during intrusion, the ultimate detachment or separation occurs most frequently at intervals of about 6 and 11 months [*Sturges and Leben*, 2000].

Hurlburt and Thompson [1980] reported the first realistic simulations of Loop Current penetration and eddy separation in a numerical ocean model of the Gulf of Mexico. The

Title
Geophysical Monograph Series

##.####/###GM##

dominant dynamical mechanism controlling the natural separation period of Loop Current eddies was found to be a horizontal shear instability of the Loop Current within the Gulf of Mexico influenced by the natural tendency of current and its associated eddies to propagate westward under the influence of β, the variation of the Coriolis parameter with latitude. An analytical model based on momentum balance considerations also highlighted the influence of β on eddy separation [*Pichevin and Nof*, 1997]. This general mechanism, which sets a natural separation period, is not the sole dynamical process controlling Loop Current penetration and eddy separation. Therefore the Loop Current exhibits a great deal of variability in the period of time between eddy separation events, which has been reported to range from 4 to 18 months [*Sturges and Leben*, 2000].

The variation of the separation period around the natural period makes it difficult to predict Loop Current penetration and eddy separation because the exact dynamical mechanisms controlling this variability are poorly understood. A popular hypothesis is that the primary source of variability around the natural Loop Current separation period comes from upstream conditions influencing the circulation within the Gulf through the connectivity of the western boundary current system in the subtropical North Atlantic gyre. This conjecture is supported by modeling studies that show anticyclonic eddies of varying origin being advected along the mean path of the upstream current system through the Yucatan channel and affecting the Loop Current behavior within the Gulf [*Murphy et al.*, 1999; *Oey et al.*, 2003]. Further support of this hypothesis comes from the vorticity flux into the Gulf calculated from in situ current measurements in the Yucatan Channel that show correlation with the changes in the Loop Current penetration and eddy separation as observed by satellite altimetry [*Candela et al.*, 2002]. The source of the vorticity flux is thought to be upstream eddies, although there is no definitive observational evidence of mesoscale eddies advecting along the Yucatan Current other than the irregular oscillations of the flow observed in the channel mooring velocity measurements [*Abascal et al.*, 2003]. Transport variations in the Loop Current [*Maul and Vukovich*, 1993], including variations in the deep outflow [*Bunge et al.*, 2002], have also been proposed as potential dynamical influences on Loop Current intrusion and eddy separation.

Another proposed mechanism for the exhibited variability is the influence of peripheral and low-layer eddies. In model simulations, a lower-layer eddy dipole pair forms beneath Loop Current rings during eddy separation [*Welsh and Inoue*, 2000] and contributes to the ultimate detachment of the eddy from the Loop Current. Simulations by *Chérubin et al.* [2004] showed that the growth of cyclones in the deep lower layer below the Loop Current recirculation are caused by an instability of the forming ring. Early in the separation process, one of the instability-generated deep cyclone pairs with a deep anticyclone to form the dipole pair inducing separation. Other studies have also noted that peripheral cyclonic eddies, including Loop Current frontal eddies [*Vukovich and Maul*, 1985], Tortugas eddies [*Lee et al.*, 1995; *Fratantoni et al.*, 1998] and Campeche Bank eddies [*Zavala-Hidalgo et al.*, 2003], are often associated with eddy separation events and are thought to play a role in the ultimate formation and detachment of a Loop Current ring.

Clearly a variety of physical mechanisms may influence Loop Current penetration and eddy separation, making identification of the dominant and/or controlling mechanisms difficult. A better understanding of the Loop Current, which is the primary source of energy and momentum driving circulation within the Gulf of Mexico [*Ohlmann et al.*, 2001], requires continuous and accurate observations. Unfortunately, Loop Current-related processes have been difficult to monitor in detail with in situ measurements and satellite imagery. Continuous monitoring of the Loop Current, however, is possible from January 1993 to the present using multi-satellite sampling provided by modern spaceborne microwave altimeters [*Leben et al.*, 2002]. Satellite altimetry is a unique remote sensing technique because it is an all-weather observing system that directly measures a dynamic variable of the ocean state, the sea surface height (SSH).

In this paper, I make a concerted effort to use the altimetric record to develop a more complete description of the Loop Current such as extent, boundary length, enclosed area, volume and circulation than has heretofore been possible using existing satellite or in situ measurement records. The time series and statistics based on these metrics provide an accurate baseline for studying the dynamical processes influencing Loop Current penetration/eddy separation and for developing realistic general circulation ocean models and prediction systems for the GOM.

2. DATA AND METHODS

A brief overview of the data sets and processing used in this altimetric study of Loop Current intrusion and eddy separation are given in this section.

Altimeter Data

The altimeter data set and processing used in this study are similar to that used in *Sturges and Leben* [2000] with several improvements. First, we have reprocessed the historical data using a new mean reference surface as described in *Leben et al.* [2002]. Second, we have incorporated altimeter data from the Jason-1, Geosat Follow-On (GFO) and TOPEX/

POSEIDON (T/P) tandem mission to improve sampling during time periods when those data are available.

Altimeter data from T/P, ERS-1&2, GFO and Jason-1 collected during the time period from January 1993 through July 2004 were used in this analysis. Standard corrections were applied to the altimeter range measurements, including inverted barometer, sea-state bias, ionosphere and wet/dry troposphere corrections. Ocean tides were removed using the tide solution derived from the Colorado Center for Astrodynamics Research (CCAR) barotropic tide model assimilating T/P data (Tierney et al., 1998).

All along-track altimeter data were referenced to the Goddard Spaceflight Center (GSFC) mean sea surface, GSFC00.1_MSS [*Wang*, 2001], which was computed using six years of T/P data, multi-years of ERS-1&2 35-day exact repeat data, Geosat 17-day exact repeat data, Geosat Geodetic Mission data, and both cycles of the ERS-1 168-day repeat data. All of the altimeter data used to calculate the mean sea surface came from the GSFC's Altimeter Pathfinder products [*Koblinsky et al.*, 1999]. After referencing the data to the mean surface, the SSH anomaly data were detrended using an along-track loess filter that removes a running least-squares fit of a tilt and bias from the along-track data within a sliding window. The window is 200 seconds along track, which is approximately 12 to 15 degrees of arc length (1200 to 1500 km). This high pass filter retains the short wavelength ocean mesoscale signals while removing the longer wavelength orbit and environmental correction errors. A consistent data set incorporating all of the available mission data is thus created by referencing the altimeter data to the same mean surface and filtering the along-track data in the manner described.

Objective Mapping

Daily analysis maps of the detrended SSH anomaly relative to the mean sea surface were estimated using an objective analysis procedure [*Cressman*, 1959] to interpolate the available along-track data to a 1/4° spatial grid. The method uses an iterative difference-correction scheme to update an initial guess field and converge to a final gridded map. A multigrid procedure provides the initial guess. Five iterations were used with radii of influences of 200, 175, 150, 125 and 100 km, while employing a 100-km spatial decorrelation length-scale in the isotropic Cressman weighting function. The data were weighted in time using a 12-day decorrelation time-scale, relative to the analysis date, using ±10-day windows on the T/P and Jason-1 data, and ±17-day windows on the ERS and GFO data. More details on the space/time-weighted multigrid preconditioned Cressman analysis are found in the Appendix to *Leben et al.* [2002].

Surface current velocity anomalies derived from these analysis maps, when compared with surface velocities from drifting buoys [*Ohlmann et al.*, 2001], demonstrate that satellite altimetry processed in this manner accurately resolves mesoscale circulation variability over the shelf rise and deep water in the western GOM. The overall goal of this work, however, is to accurately monitor the Loop Current penetration and eddy separation, which requires accurate estimation of both the mean and time varying signal in the eastern GOM. This is described in the next section.

Loop Current Monitoring

Altimetric monitoring of the Loop Current is difficult because of the large contribution of the mean circulation to the total dynamic topography in the eastern GOM. Although altimeter systems measure variations in SSH very accurately, imprecise knowledge of the marine geoid makes accurate absolute measurements of the total sea surface topography associated with ocean circulation at mesoscale wavelengths impossible at this time. Synthetic observations of the total dynamic topography, however, can be constructed by adding an independent estimate of the mean sea surface height to the height deviation measured by altimeter satellites relative to a long-term altimetric mean.

To calculate the synthetic SSH estimates used in this study, we selected a model mean sea surface height computed for the time period 1993 through 1999 from a data assimilation hindcast performed by Drs. Lakshmi Kantha and Jei Choi for the MMS Deepwater Physical Oceanography Reanalysis and Synthesis Program [*Nowlin et al.*, 2001] using the University of Colorado-Princeton Ocean Model (CUPOM). Along-track TOPEX and ERS-1&2 sea surface height anomalies were assimilated into CUPOM on a track-by-track basis as subsurface temperature anomalies (see the paper by *Kantha et al.*, this volume). Before adding the model mean to the gridded SSH anomaly fields we averaged the 1993 through 1999 SSH anomaly fields and removed the residual anomalous altimetric mean. This references the SSH anomaly fields to a mean spanning the same time period as determined from the model hindcast data assimilation experiment. The anomalous altimetric mean reflects the difference between the mean circulation contained in the GSFC mean sea surface and the 1993-1999 model mean. More discussion of these differences is found in *Leben et al.* [2002].

The qualitative differences in synthetic maps created using various model and climatology means are not very remarkable; however, derived quantitative metrics can be sensitive to the mean selected. For example, the sensitivity of the analysis of eddy separation determined from the altimetric record [*Sturges and Leben*, 2000] was found to

have little dependence on the mean added to the altimeter-derived sea surface height anomalies. Quantitative Loop Current metrics, which I describe in the next section, show more sensitivity to the mean used to estimate the synthetic height. The fidelity of these estimates was evaluated by comparing individual synthetic height maps with coincident satellite imagery. In that preliminary qualitative study, I found that robust metrics could be determined when using the CUPOM data assimilation model mean with referencing of the altimeter data record to a mean computed over the data assimilation time period.

Loop Current Metrics

Having a synthetic estimate of the mean plus dynamic height, it is feasible to objectively track the Loop Current in the GOM SSH maps. In *Hamilton et al.* [2000], I described a novel Loop Current monitoring capability provided by satellite altimetry that uses the 17-cm SSH contour as a proxy for the high velocity core of the Loop Current in the eastern GOM. This proxy allows objective calculation of a variety of Loop Current metrics such as the length, area, volume and circulation associated with the Loop Current penetration into the Gulf, and its maximum northward and westward extent. The metric time series can then be used to objectively identify Loop Current eddy separation periods, the time intervals between eddy separations.

The use of the 17-cm contour was based on our early success tracking Loop Current rings using altimetry [*Leben and Born*, 1993]. Altimetric monitoring of Loop Current rings in the western Gulf of Mexico relies on the small contribution of the mean circulation to the total dynamic topography. In *Berger et al.* [1996], the 17-cm SSH anomaly contour was selected to derive quantitative metrics for the Loop Current eddies because the contour closely matched the location of maximum gradients in the surface topography corresponding to the edge of the high-velocity core of the eddies. This allowed continuous tracking of Loop Current rings during their translation through the western Gulf of Mexico. The 17-cm contour of total dynamic topography (SSH plus mean) also works well as a definition for the outer edge of the high-velocity core of the Loop Current in the eastern Gulf of Mexico (Plate 1).

The procedure for computing the metrics from the SSH fields has been automated by a MATLAB® program that accesses a GOM altimeter data archive and computes the values. Daily values for each metric are computed using the following algorithm:

1. Load the 0.25° gridded SSH field and generate the coordinates of the 17-cm contours within the Gulf.
2. Identify the Loop Current core, which is defined as the continuous 17-cm contour that enters the gulf through the Yucatan Channel and exits through the Florida Straits.
3. Find the maximum west longitude and north latitude coordinates to determine the extent of westward and northward penetration of the Loop Current.
4. Compute the length of the Loop Current by summing the distances between the coordinates on the 17-cm contour.
5. Identify all 0.25° grid cells bounded by the 17-cm contour and compute the total Loop Current area by summing the areas of the individual cells.
6. Estimate the Loop Current volume, assuming a one and a half-layer ocean and a reduced gravity approximation, by evaluating the following area integral over the region bounded by the 17-cm contour:

$$\iint \frac{g}{g'} h dx dy,$$

where h is the sea surface height; g is the acceleration of gravity; and g' the reduced gravity. (A value of 0.03 m/s^2 was used for g'.)

7. Estimate the Loop Current circulation by the line integral of the geostrophic velocity along the 17-cm contour:

$$\oint \vec{V} \cdot ds = \int u dx + \int v dy,$$

where u and v are the geostrophic velocity components and dx and dy are the coordinate spacing in the east/west and north/south directions, respectively. The geostrophic velocity components at the midpoint locations are found by bilinear interpolation from the gridded geostrophic velocity components computed from the height field. (The sign convention employed here is such that the anticyclonic vorticity associated with the Loop Current is positive and therefore in positive correlation to the other metrics.)

The most difficult computational aspects of the algorithm are the autonomous tracking of the Loop Current contour in the presence of any other contours (such as those associated with detached Loop Current eddies) and identifying the Loop Current grid cells within the tracking. Otherwise, this is a relatively simple algorithm to implement using existing contouring programs and could be used to compute similar metrics from numerical ocean model experiments. These metric and their statistics would be useful for parametric tuning and/or model skill assessment. The Loop Current tracking contour, however, typically will be different for each model implementation.

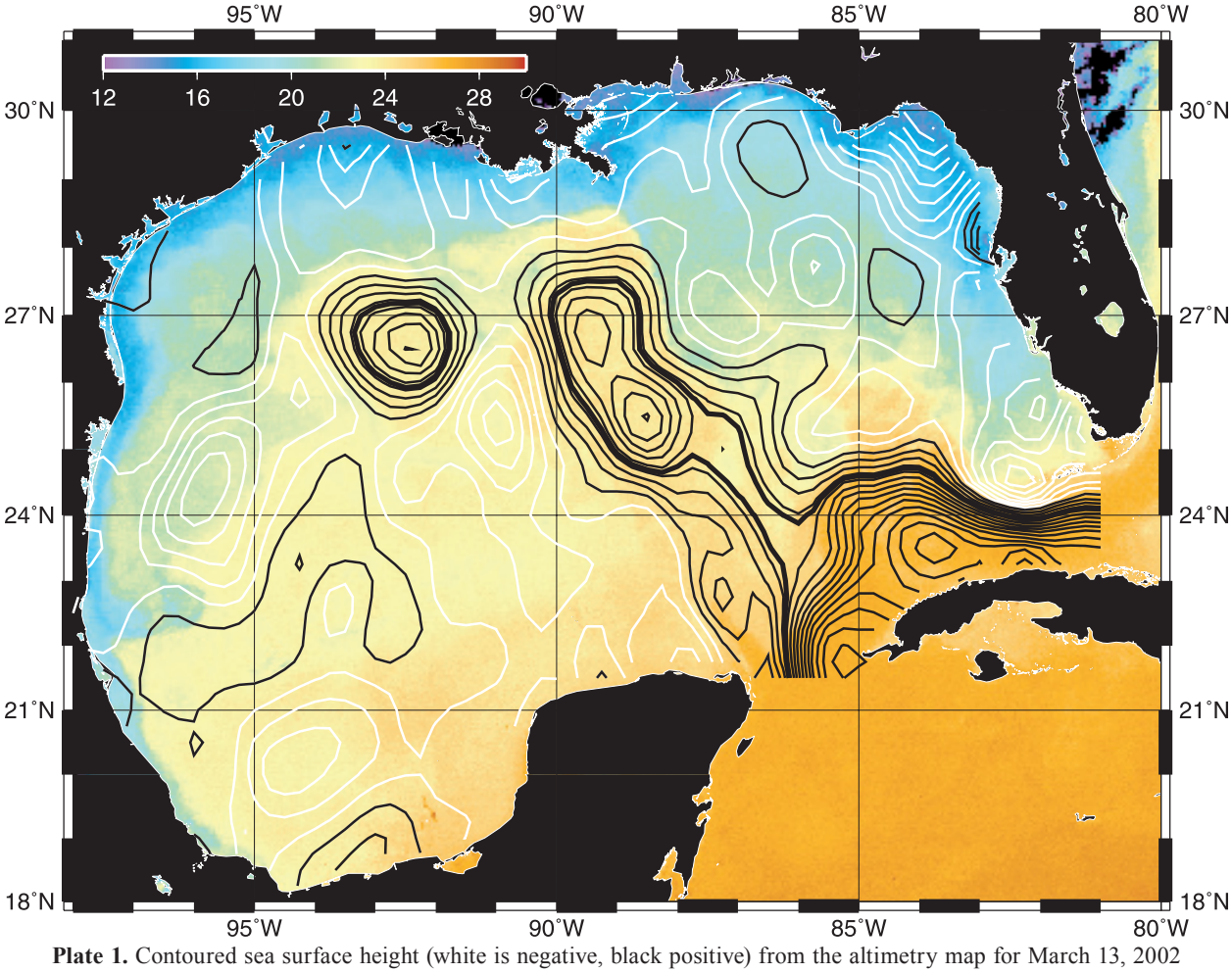

Plate 1. Contoured sea surface height (white is negative, black positive) from the altimetry map for March 13, 2002 overlaid on the nighttime composite SST image from the GOES 8 satellite for the same day (courtesy of Nan Walker, Louisiana State University). The 17-cm contour used to track the Loop Current boundary and eddies is shown by the bold line. The westernmost eddy (Pelagic Eddy or Eddy 13) separated from the Loop Current on February 28th, followed closely by a second eddy (Quick Eddy or Eddy 14) on March 15th, using the objective criteria of breaking of the 17-cm contour.

3. RESULTS

Loop Current statistics [*SAIC*, 1989] and the eddy separation cycle [*Vukovich* 1988; 1995]; *Sturges,* 1992, 1994; *Vukovich,* 1995; *Sturges and Leben,* 2000] have been studied in some detail; however, the analysis has been limited by the available observations and by the difficulty in defining a separation event objectively. In this section, I use the continuous 11.5-year altimeter data record and the Loop Current tracking algorithm to describe the Loop Current in much greater detail than possible before tandem altimetry sampling became available starting in 1993.

Loop Current Metrics: Time Series and Statistics

The GOM SSH data archive and Loop Current tracking algorithm were used to compute Loop Current metric values for the time period from 1 January 1993 through 1 July 2004. Time series of Loop Current maximum latitude/longitude extension and length are shown in Plate 2 and area, circulation, and volume in Plate 3. Histograms of the distributions and mean values are shown in the lower panels. Summary statistics for each of the metrics are shown in Table 1.

The total area of open water on the 1/4°grid in the Gulf of Mexico is 1,512,000 km^2. During this time interval, the average area covered by the Loop Current was 147,240 km^2 or approximately 10% of the Gulf. The average length was 1376 km and average circulation was 1,396,200 m^2/s. The total estimated Loop Current volume was 2.26×10^{13} m^3. This volume would take over eight days to fill assuming an average inflow of 30 Sv, which is typical of the transport into the Gulf through the Yucatan Channel. The average maximum northward and westward extension of the Loop Current intrusion were 26.2°N and 87.9°W. The maximum and minimum northward extension into the Gulf observed during the time interval were 28.1°N and 24.1°N, respectively. The maximum and minimum westward extension were 93.1°W and 85.8°W. These statistics are quite stable; the Loop Current statistics from this 11.5-year time series differ very little from similar statistics computed from an 8.33-year altimetric record that was reported in *Hamilton et al.* [2000]. This is further confirmed by the good agreement between the standard deviation of the Loop Current northern boundary reported by *Maul and Vukovich* [1993] with the altimeter-derived result. They report a 102 km standard deviation of the northern boundary location for the time period from 1977 through 1988, compared to 106 km reported here (0.95 degrees) using the altimeter record.

Loop Current statistics have also been derived from 10 years (1976–1985) of monthly frontal analysis maps based on AVHRR thermal images [*SAIC*, 1989]. The summary statistics from that study reported an average area of 210,000 km^2 and 29.75°N and 91.25°W for the maximum northward and westward extensions. The average area derived from thermal imagery was nearly 50% larger than the altimetric estimate reported here. This difference is attributable to the offset between the surface thermal fronts and the location of the Loop Current boundary determined from altimetry. A similar offset of 50 to 100 km was found between the surface frontal analysis maps and subsurface temperature gradients at 125 meters determined from coincident XBT survey transects [*SAIC*, 1989]. Assuming that the mean Loop Current statistics over the two observation intervals are comparable (i.e., stationary), the relative offset can be estimated by the difference of the averages divided by the average length of the Loop Current. This gives an estimate of approximately 45 km for the offset. The integrated effect of this offset is to make estimates of the Loop Current areal extent from thermal imagery significantly larger than values determined using the altimetric Loop Current tracking procedure described herein.

The matrix of correlation coefficients computed from the time series of Loop Current metrics is shown in Table 2. Identifying a "best" metric for monitoring the Loop Current is difficult because of the high correlation between the individual time series. Dynamical considerations may favor the circulation metric, which shows the most consistent growth throughout an intrusion event and the greatest increase just before separation. Loop Current volume and maximum westward extent are the least correlated with the other metrics and

Table 1. Summary statistics for the Loop Current metrics (see Plates 2 and 3) computed from the 1 January 1993 through 1 July 2004 altimetric time series.

	Maximum West Longitude	Maximum North Latitude	Length	Area	Volume	Circulation
Mean	87.9°W	26.2°N	1376 km	147,240 km^2	2.26×10^{13} m^3	1,396,200 m^2/sec
Std. Dev.	1.18°	0.95°	365 km	29,295 km^2	0.37×10^{13} m^3	338,960 m^2/sec
Maximum	93.1°W	28.1°N	2494 km	213,540 km^2	3.08×10^{13} m^3	2,311,200 m^2/sec
Minimum	85.8°W	24.1°N	614 km	55,840 km^2	0.85×10^{13} m^3	611,420 m^2/sec

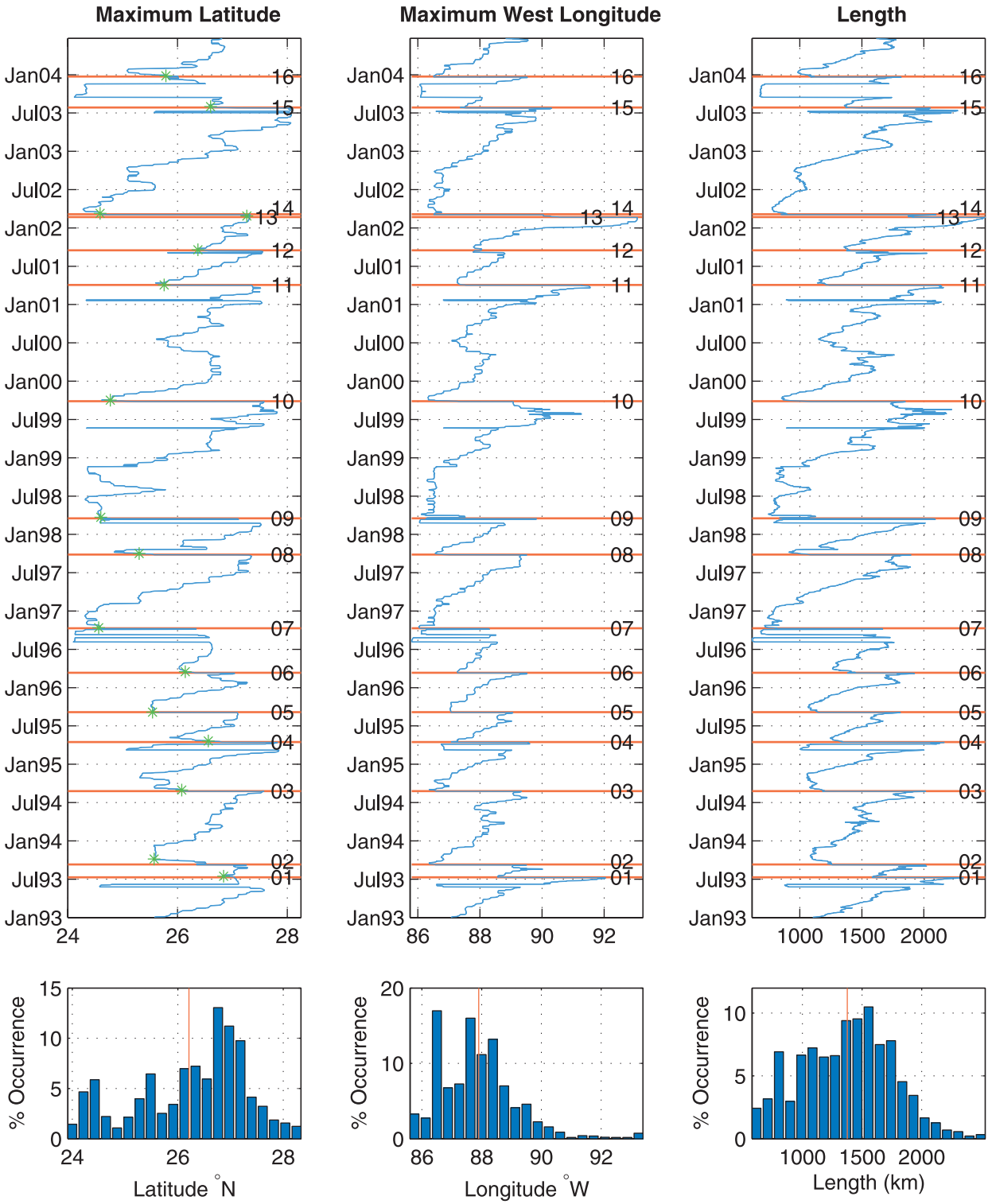

Plate 2. Loop Current maximum northern/western extension and length time series from the altimeter record based on tracking of the 17-cm contour are shown in the upper panels. The horizontal red lines identify the 16 Loop Current eddy separation times. Percent occurrence histograms are shown in the lower panels. Vertical red lines overlaid on the histograms show the mean values (see summary statistics in Table 1 for values).

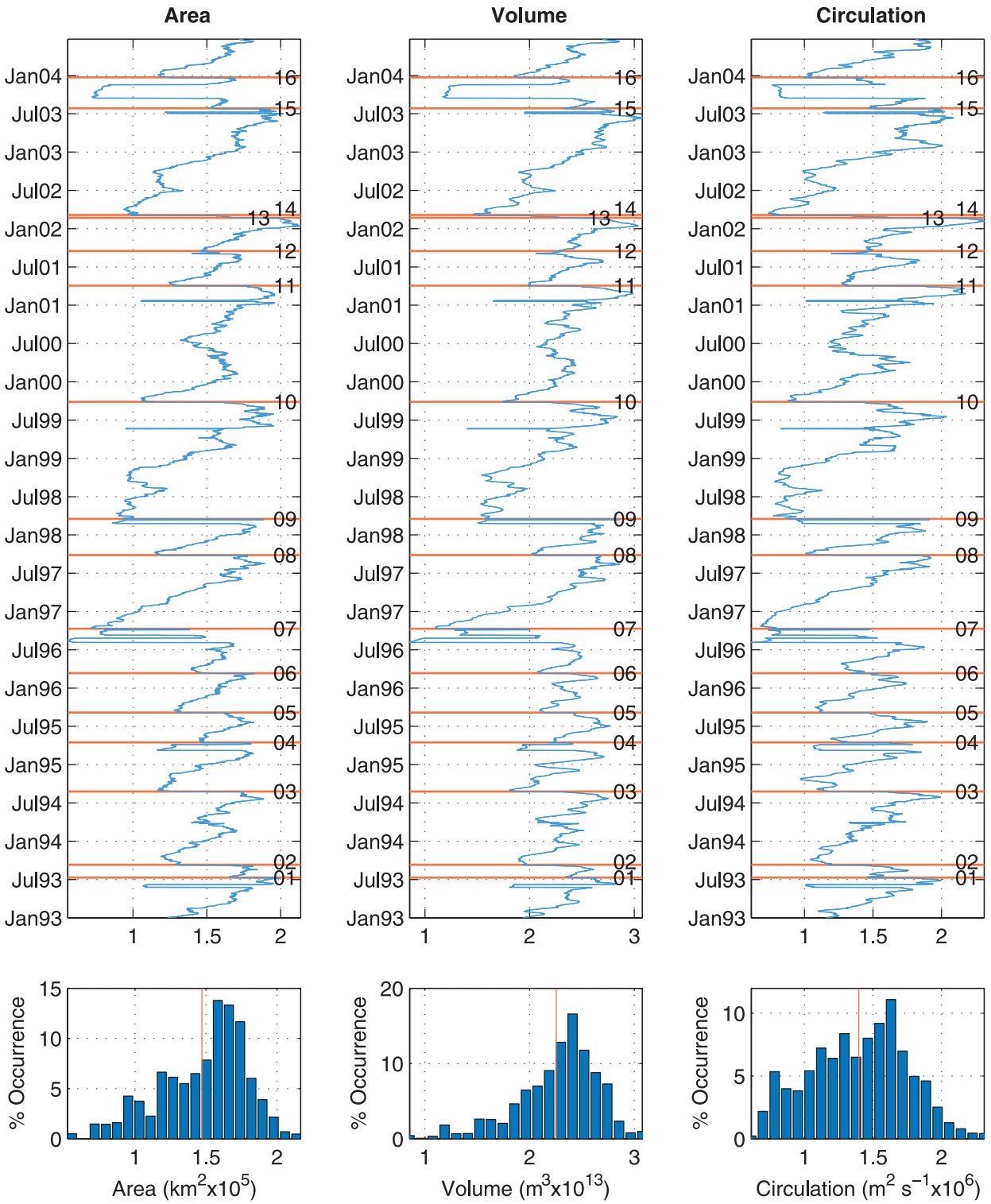

Plate 3. Loop Current area, volume and circulation time series from the altimeter record based on tracking of the 17-cm contour are shown in the upper panels. The horizontal red lines identify the 16 Loop Current eddy separation times. Percent occurrence histograms are shown in the lower panels. Vertical red lines overlaid on the histograms show the mean values (see summary statistics in Table 1 for values).

Table 2. Correlation Matrix for Loop Current Metrics

	Area	Volume	Circulation	Maximum North Latitude	Maximum West Longitude	Length
Area	1.00	0.95	0.93	0.95	0.89	0.95
Volume	0.95	1.00	0.90	0.88	0.80	0.85
Circulation	0.93	0.90	1.00	0.91	0.88	0.94
Max. North Lat.	0.95	0.88	0.91	1.00	0.81	0.94
Max. West Lon.	0.89	0.80	0.88	0.81	1.00	0.94
Length	0.95	0.85	0.94	0.94	0.94	1.00

exhibit larger variations independent of separation events. I prefer to use the Loop Current length. The high correlation found between the altimeter-derived metrics, however, supports the use of surrogate time series as proxies for shedding events. For example, there is very high correlation between area, length and circulation and the northward penetration of the Loop Current, a metric that could easily be computed from model simulations. There has been one estimate of the correlation coefficient between area and northward extent of the Loop Current reported, which is based on frontal analysis derived from the thermal imagery [*SAIC*, 1989]. The value found was 0.76. This is significantly less than the 0.95 determined from the altimetric analysis and may be related to the difficulties associated with identifying the Loop Current boundary in thermal imagery and the smoothing inherent in the processing of the altimeter data. A more detailed comparison of these two remote sensing techniques is described in the next section.

Loop Current Metrics: Comparisons with Satellite Imagery

Direct comparisons of the Loop Current thermal fronts seen in SST imagery with the Loop Current position determined using the synthetic altimetry product (SSH anomaly plus mean) were made to evaluate the Loop Current tracking technique. The Loop Current 17-cm tracking contour was overlaid on SST images sampled during times of good thermal contrast and cloud free conditions. In general, the qualitative agreement is quite good, with the 17-cm contour tracking the Loop Current front within a relatively consistent offset to the inside of the surface thermal front as seen in the imagery (e. g., see Plate 1).

To quantify the offset between the 17-cm contour and the surface thermal front, I made a direct comparison of the location of the 17-cm contour relative to the SST front at the northernmost point of the Loop Current intrusion. Five-day composite SST images from 1993 through 1999 [*Casey and Cornilon*, 1999] coincident with the altimeter maps were sampled along longitude meridians within +3° and -2° degrees of the point of maximum northern intrusion of the 17-cm contour of SSH. The agreement is good during times of strong thermal contrast; however, the 17-cm contour is consistently south of the SST front. Tracking this offset in the thermal imagery is difficult because of seasonal variations in the thermal signature of the Loop Current and surface waters north of the Loop Current. Nevertheless, during times of good thermal contrast, the maximum temperature gradient is a robust locator of the Loop Current front with the maximum absolute values of the north/south gradient corresponding to the location of the front. Mean values of the north/south temperature gradient as a function of position relative to the 17-cm Loop Current contour are used to quantify the relative offset. The largest negative mean gradient values are located to the north of thermal front, with little mean gradient to the south over the nearly isothermal Loop Current waters (Figure 1). The extrema value of the mean gradient is offset north of the Loop Current tracking contour by 0.44° of latitude. This is approximately 50 km and in very good agreement with the back-of-the-envelope estimate described in the previous section for the offset between the tracking contour and the surface thermal front. The variability about this bias offset is remarkably small, given the occurrence of warm water filaments and other fine scale frontal variations on the periphery of the Loop Current that are not well sampled by the altimeters. No comparisons can be made, however, during much of the time period, which highlights the difficulty of continuously monitoring the Loop Current with thermal imagery alone.

Loop Current Penetration and Eddy Separation

A primary reason for computing objective metrics is to monitor the time-dependent behavior of the Loop Current system as it intrudes and sheds rings, which are the dominant source of the upper ocean circulation variability in the deep GOM. Clearly a Loop Current intrusion and eddy separation event is associated with each of the peaks in the

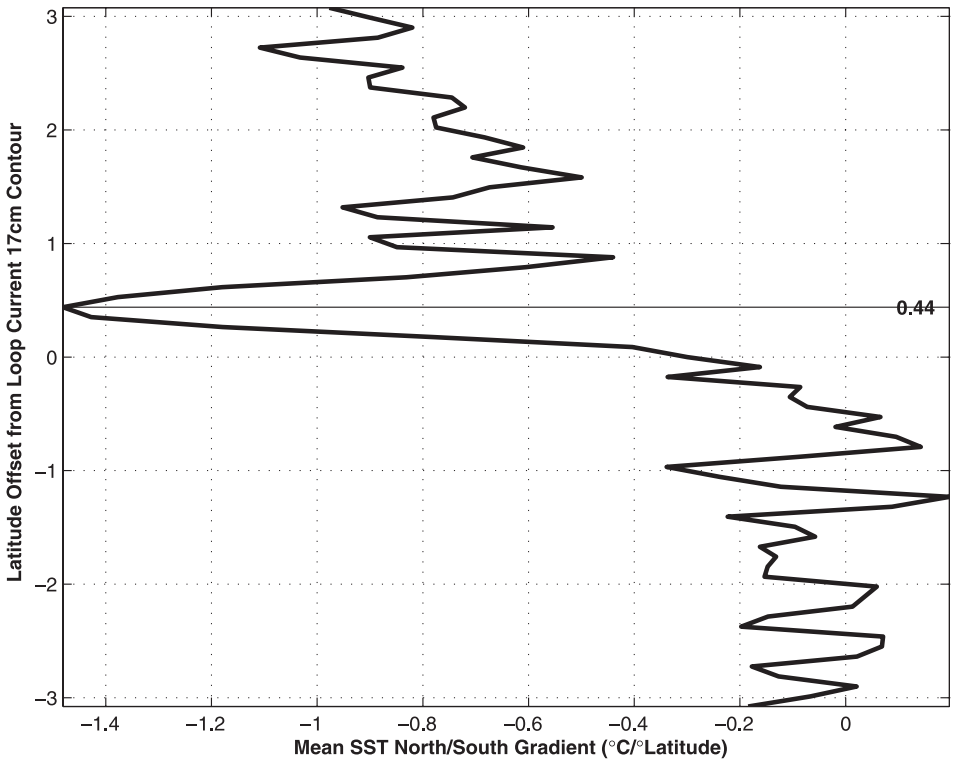

Figure 1. The mean north/south gradient of SST is shown as a function of the latitude offset relative to the northernmost point of 17-cm SSH contour tracking the Loop Current position. The extrema value corresponding to the offset between the surface thermal front and the 17-cm tracking contour is 0.44° of latitude, or approximately 50 km.

metric time series shown Plates 2 & 3. The exact timing of the event, however, is dependent on the criteria selected for the definition of separation, which in turn ultimately defines what counts as a Loop Current eddy. This exercise is further complicated by the ambiguity of associating an exact time with what is clearly a continuous and complicated process. Nevertheless, an objective definition greatly simplifies monitoring of Loop Current eddy separation and comparing observations with dynamical theories and/or model simulations.

We identify timing of Loop Current eddy separation events using the Loop Current length time series since the breaking of 17-cm contour between the Loop Current and a detaching eddy into separate contours causes a discrete change in Loop Current length equal to the circumference of the eddy. The day that this event occurs is identified as the "time" of eddy separation. In cases where the eddy subsequently reattaches to the Loop Current, the final detachment time is used. This requires manual discrimination, which means that identifying separation events cannot be completely automated. The time series of SSH maps must be used to differentiate between cases where an eddy reattaches or two eddies separate within a short time period; nevertheless, the separation events are identified objectively since the two cases are easily distinguished. The separation events so identified are shown on each of the subplots of the metric time series in Plates 2 and 3. The Loop Current length time series and SSH maps of each of the sixteen eddy separation events at the time of final detachment in the 1993 through 2003 record are shown in Plate 4.

In Table 3, the date of final detachment, separation period, name and eddy area at the time of separation are tabulated for each of the 16 observed events. Horizon Marine, Inc. (HMI) names the eddies in alphabetical order as anticyclones shed from the Loop Current and/or impact offshore operations in the northern GOM. A complete list to date is located on the web at http://horizonmarine.com/namedlces.html. The names appear in the weekly EddyWatch™ reports provided to the GOM offshore oil and gas industry by subscription from HMI. All separation events identified using the SSH 17-cm tracking contour were monitored by the EddyWatch™ program, although a number of smaller anticyclonic eddies (7 total) were also named, causing the breaks in the alphabetical sequence. Only one marginal eddy separation event was identified by the objective tracking procedure (Eddy Odessa/Nansen, Eddy 12), which dissipated so quickly that an area estimate for the eddy

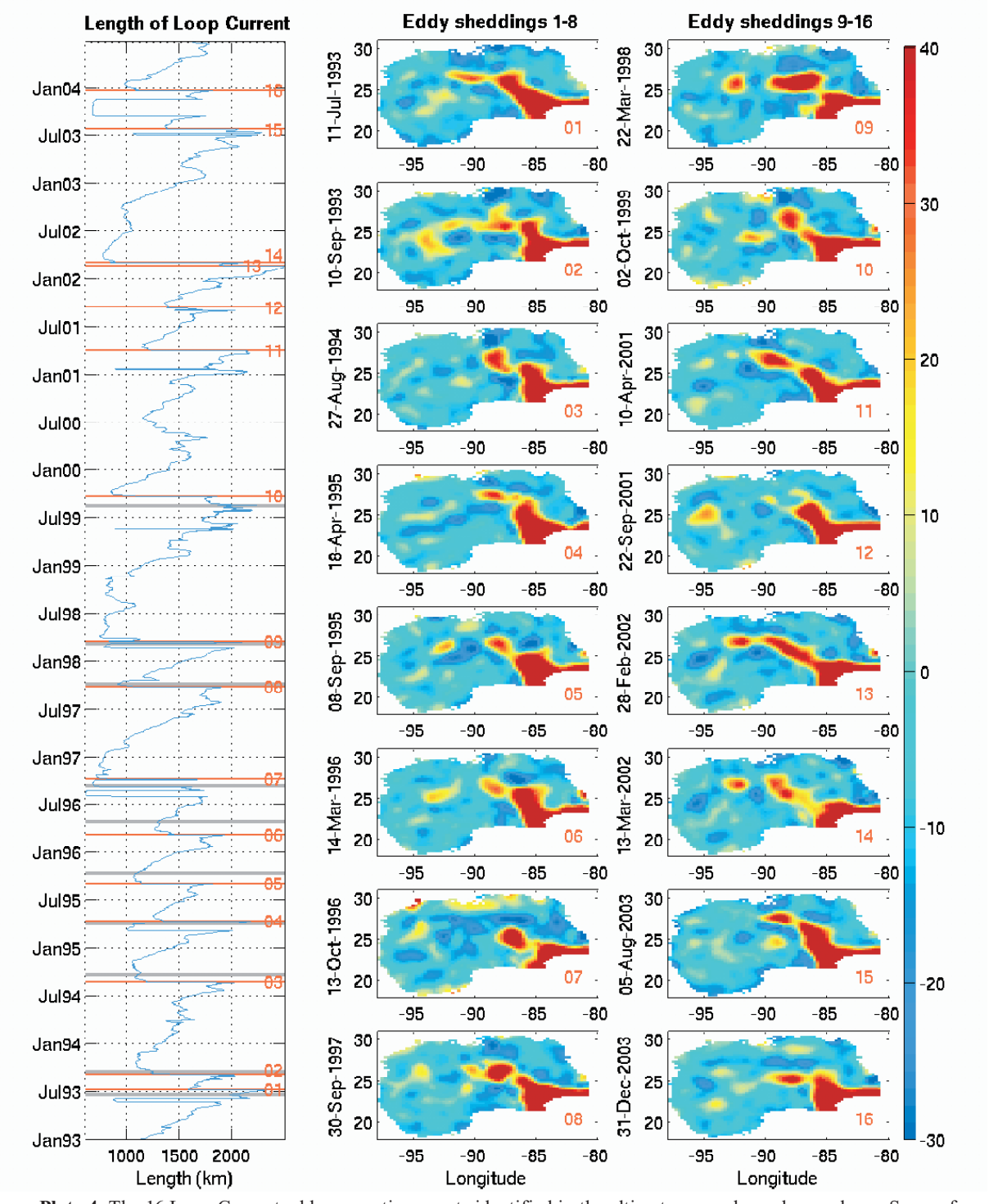

Plate 4. The 16 Loop Current eddy separation events identified in the altimeter record are shown above. Sea surface height maps on the separation dates are shown in the panels to the right (note that the values above 40 cm and below -30 cm have been clipped). Eddy separation times were objectively determined by breaking of the 17-cm tracking contour, which causes a discrete change in the Loop Current length (left panel). The length time series is overlaid with red lines corresponding to the 16 events identified. Gray lines show the 10 separations times determined using the subjective method described in *Sturges and Leben* [2000].

Table 3. Ring separation events from altimetric record 1993-2004. The Eddy Ulysses separation date (*) is a subjective estimate based on imagery and near real-time altimetry.

Eddy Number	Date	Separation Period (months)	Industry Eddy Name	Area (km^2)
1	11 Jul 1993	11.5	Whopper	24,183
2	10 Sep 1993	2.0	Xtra	38,481
3	27 Aug 1994	11.5	Yucatan	43,022
4	18 Apr 1995	7.5	Zapp	21,337
5	8 Sep 1995	4.5	Aggie	24,899
6	14 Mar 1996	6	Biloxi	24,912
7	13 Oct 1996	7	Creole	49,644
8	30 Sep 1997	11.5	El Dorado	49,229
9	22 Mar 1998	5.5	Fourchon	89,143
10	2 Oct 1999	18.5	Juggernaut	40,325
11	10 Apr 2001	18.5	Millennium	45,705
12	22 Sep 2001	5.5	Odessa/Nansen	?
13	28 Feb 2002	5.5	Pelagic	22,119
14	13 Mar 2002	0.5	Quick	49,936
15	5 Aug 2003	17	Sargassum	25,302
16	31 Dec 2003	5	Titanic	33,278
17	*15 Sep 2004	9.5	Ulysses	

could not be made. These smaller eddies are of Loop Current origin, but form on the outer edge of the Loop Current through the interaction of frontal cyclones with the current. This type of small anticyclonic eddy was observed in the northeast GOM during the DeSoto Canyon Eddy Intrusion Study [*Hamilton et al.*, 2000]. Other small named eddies originate as primary Loop Current eddies split and/or shed smaller anticyclonic eddies after separation.

Several notable Loop Current events occurred in the altimeter record. Seven of the sixteen eddies (Eddies 1,4,7,9,11,15, and 16) detached and reattached before final separation. Most of these were short lived; however, a two-month long detachment/reattachment period occurred in the fall of 2003 before the separation of Eddy 16 from the Loop Current. During this detachment event, the interaction of the detached anticyclone with the strong cyclone to the north may have arrested the westward β-induced drift through the eastward velocity induced by the dipole pair formed by the cyclone to the north and the detached anticyclone to the south. The shortest eddy separation period (two weeks) is associated with the first observations of a nearly simultaneous separation of two eddies from the Loop Current. These selected events and other details can be examined in the 11.5 year-long SSH animation included on the CD-ROM accompanying this monograph.

In Table 4, I compare the subjective ring separation dates published in *Sturges and Leben* [2000] with the objective estimates derived using the 17-cm LC tracking contour for the overlapping events considered. The subjective ring separation dates are also plotted on the Loop Current length time series (see gray lines in left panel of Plate 4). The subjective estimates were found by simply examining each SSH map to determine whether a ring appeared to be separating and continuing to track the separation process until completion. The midpoint of the separation process was identified as the time of separation and an expected uncertainty was assigned based on the duration of the separation process. The average difference in the subjective versus objective separation dates was only three days because of the canceling of differences from event to event. The standard deviation (std) of the differences (29 days) is in good agreement with the root mean square (rms) of the subjective technique uncertainty estimate, which is about 3.5 weeks or 25 days. This is a more robust comparison of the two methods and shows that event tracking

Table 4. Comparison of *Sturges and Leben* [2000] subjective ring separation dates and periods with the objective estimates based on the 17-cm Loop Current tracking contour.

	Sturges and Leben (2000)			17-cm contour results		
Event	Date	Separation Period (months)	Uncertainty (weeks)	Date	Separation Period (months)	Date Difference (days)
1	22 Jun 1993	11	4	11 Jul 1993	11.5	-19
2	19 Sep 1993	3	1	10 Sep 1993	2	9
3	22 Sep 1994	12	4	27 Aug 1994	11.5	26
4	8 Apr 1995	7	4	18 Apr 1995	7.5	-10
5	18 Oct 1995	6	4	8 Sep 1995	4.5	40
6	30 Apr 1996	6	5	14 Mar 1996	6	47
7	Sep 1996	5	4	13 Oct 1996	7	-28
8	11 Oct 1997	13	3	30 Sep 1997	11.5	11
9	14 Mar 1998	5	2.5	22 Mar 1998	5.5	-8
10	22 Aug 1999	17	2	2 Oct 1999	18.5	-41
	Mean	8.5			3	3
	Standard Deviation	4.5	3.5 rms		4.8	29

within the uncertainty of an expert/subjective technique can be obtained with the objective technique. There is less scatter in the subjective versus objective separation period (4.5 versus 4.8 month std., respectively), which is presumably caused by subjective smoothing of separation times when evaluating the SSH maps within the separation window.

A histogram of the updated distribution is shown in the upper panel of Figure 2. The 16 events that occurred during the altimetric record are shown in dark gray to highlight the contribution of the more recent events to the histogram of the complete observational record. The histograms of events before and after 1993 are shown in the middle and lower panels, respectively. The mean for the entire compilation is 9.4 months and the mode is 6 months. Using only the pre-1993 record, the mean is 9.96 and the mode is 6 and 9 months, whereas for the altimeter-derived objective tracking periods the mean is 8.6 months and the mode is 6 and 11.5 months. These differences are probably not significant; nevertheless, the change in the distributions between the earlier time period and the altimeter record is striking (see the histograms shown in the lower two panels of Figure 2). This attests to the remarkable variability of the Loop Current eddy separation period.

Loop Current Spectral Analysis

Next I evaluate the subjective versus objective Loop Current tracking technique for estimating the Loop Current spectrum. One method to compute the periodicity of the Loop Current eddy separation is the histogram technique described by *Sturges* [1994]. In this method, a histogram of ring separations is plotted as a function of the inverse separation interval eddy separation cycle to resemble a variance-preserving power spectrum. Hanning passes are used to smooth the distribution while retaining high resolution. The distributions based on the 34 consecutive separation events (1973-1999) as published in *Sturges and Leben* [2000] and an updated version, including the 16 altimeter-derived objective eddy separation intervals through 2003 [a total of 40 consecutive events (see Table 5)], are shown in Figure 3. Both distributions have been smoothed with two Hanning passes.

As expected, the distributions are not much different because of the substantial amount of shared information between the two data sets. Primary peaks in the distributions are found at 6, 9 and 11 months. The one notable difference between the two distributions is the peak appearing near 18 months. More power is seen at this frequency in the smoothed histogram calculated from the extended time series because of the additional events, including two 18.5-month separation periods. The original time series had a maximum separation period of 17 months and only one event of that duration. All of these long-period events occurred after 1998.

The primary limitation of the histogram technique is that, by using only separation periods to estimate the spectrum, no power below the frequency associated with the maximum separation period in the record can be observed. This limits the spectrum to periods less than about 18.5 months for the existing Loop Current observations. By focusing on ring

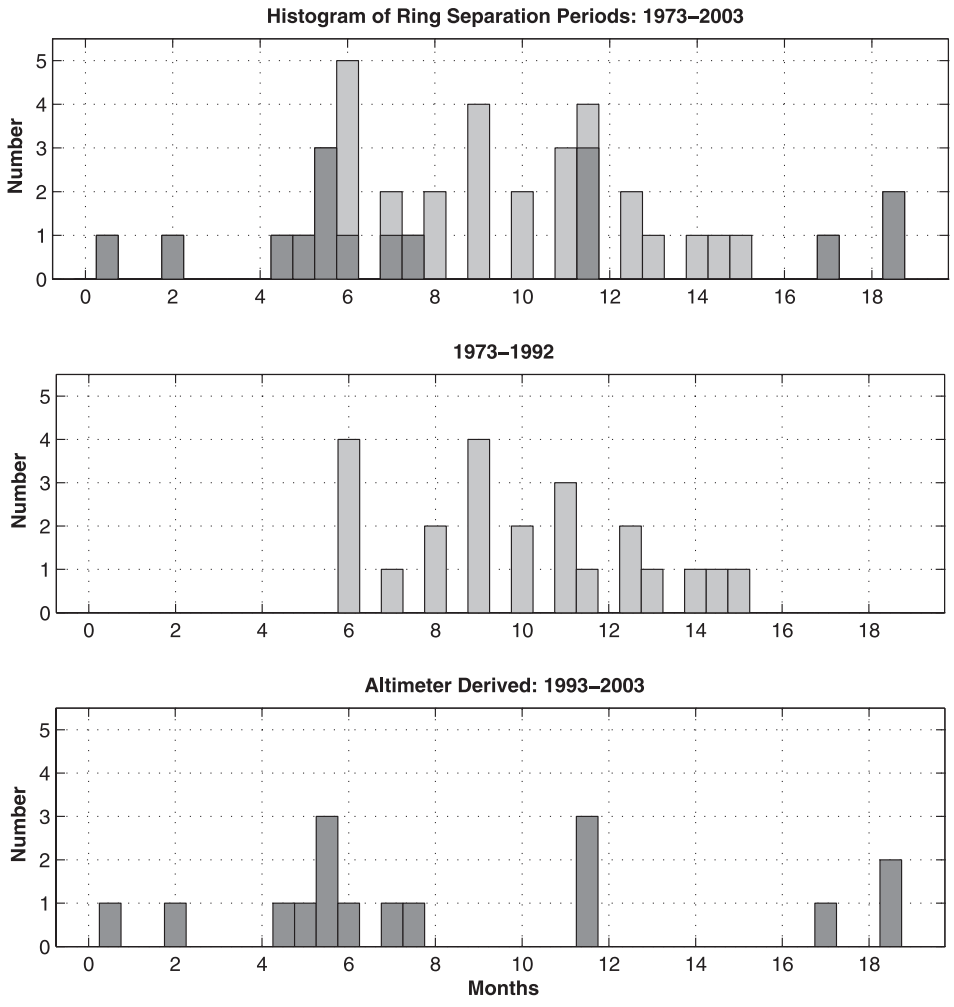

Figure 2. Histogram of the times between ring separations using the data from Table 5 are shown for selected time intervals. The 16 separation events observed during the satellite altimeter record are shown in dark gray, the prior separations in light gray. The range of periods is from 0.5 to 18.5 months, with a mean of 9.4 months and a mode of 6 months.

separations times, one effectively filters the power at all frequencies that are associated with the variability of the Loop Current envelope independent of eddy separation and gives unit power to each individual separation event. This is a reasonable analysis if one is concerned only with the frequency of eddy separation events. More information, however, can be obtained from the spectrum of a continuous time series. For example, the spectrum of the Loop Current length time series contains information on both the frequency and power of the Loop Current length but also the implicit changes in length caused by eddy separation.

The altimeter-derived Loop Current length time series spectrum is shown in Figure 4. Before computing the spectrum, the mean and trend were removed from the 4201 daily values and a full Hanning window taper was applied to the time series to reduce end effects and leakage. Similar to the histogram spectra (Figure 3), there are peaks in the length spectrum at 6, 9 and 11.5 months and little power at exactly 12 months. The dominant peak, however, is at 22 months. This power is associated with both long-period eddy separation events and the far south retreat of Loop Current preceding those separation that cause a very strong low frequency signal in the length time series. This merits further analysis.

A cursory examination of the altimeter-derived metrics finds an apparent relationship between the Loop Current retreat following eddy separation and the subsequent eddy separation period. The far southern retreats are associated with longer separation periods. This is shown in Figure 5. Eddy separation periods are plotted versus the values of

Table 5. A compilation of the 31-year record (July 1973 through June 2004) of LC eddy separation events. A total of 40 consecutive events are listed. Entries through Oct 1986 are from *Vukovich* [1988]; other entries prior to July 1992 are from Table 1 of *Sturges* [1994] using corrections based on *Berger* [1993]. The event in July 1992 is from *Sturges and Leben* [2000]. Data beginning in 1993 are based on objective tracking of the Loop Current using satellite altimeter data, this study.

Date	Separation Period (months)	Date	Separation Period (months)
July 1973		May–June(?) 1989	12.5
April 1974	9	August 1990	14.5
January 1975	9	Aug–Sep 1991	12.5
July 1975	6	19 July 1992	11.5
August 1976	13	11 Jul 1993	11.5
March 1977	7	10 Sep 1993	2
June 1978	15	27 Aug 1994	11.5
April 1979	10	18 Apr 1995	7.5
January 1980	9	8 Sep 1995	4.5
March 1981	14	14 Mar 1996	6
November 1981	8	13 Oct 1996	7
May 1982	6	30 Sep 1997	11.5
March 1983	10	22 Mar 1998	5.5
February 1984	11	2 Oct 1999	18.5
August 1984	6	10 Apr 2001	18.5
July 1985	11	22 Sep 2001	5.5
January 1986	6	28 Feb 2002	5
October 1986	9	13 Mar 2002	0.5
September 1987	11	5 Aug 2003	17
May 1988	8	31 Dec 2003	5

the Loop Current northern extent (Loop Current maximum latitude) immediately following the previous eddy separation event. These northern Loop Current extent values were calculated by finding the minimum value of the Loop Current 17-cm contour maximum latitude coordinate in the five-day window following separation of a Loop Current eddy. The values are also plotted overlaid on the maximum latitude time series (see green stars in left panel of Plate 2). I elected to edit the latitude of one retreat value (number 3 at 26.34°N) that did not reflect the initial state of the Loop Current because in that event a warm filament affected the 17-cm tracking contour just after eddy separation. Instead, I choose a value of 25.6°N that corresponds to the latitude where the Loop Current remained for nearly three months just after separation. Otherwise, the Loop Current retreat values are relatively stable and can be calculated in a variety of ways by using mean or extrema values within a variety of windows.

There is a distinct break in the distribution of values near the retreat latitude of 25°N. This break is also reflected in the overall distribution which shows a bimodal distribution centered at 25°N in the histogram of the Loop Current maximum latitude (lower left panel of Plate 2). During this time period from 1993 through 2003, the average separation period following retreat is 16.2 months when the entire Loop Current retreats to below 25ºN, much longer than the 5.5 month average for the cases where part of the Loop Current remains north of 25ºN. Above about 26ºN, there is a strong linear relationship between period and retreat with the exception of event 3, which has already been discussed. Below 26ºN there is more scatter in the data, most notably events 6, 8, 9, and 12; nevertheless, the overall correlation of retreat to period is –0.88 (-0.83 with unedited point number 3).

Investigation of the incongruent period associated with separation event 8 leads to an interesting relationship. While events 10, 11 and 15 are clustered along the line extrapolating the nearly linear relationship of retreat to period above 26ºN, the period associated with event 8 is much shorter. Note, however, that if the periods of events 8 and 9 are combined and plotted with the initial retreat of event number 8, then the point falls within the cluster of the other three southernmost retreat points. In fact, if all of the events exhibiting the incongruent periods (events 6, 8 and 12) are combined with the period of the next eddy separation event (events 7, 9, and 13, respectively), then a nearly perfect linear relationship is found between retreat latitude and separation period (Figure 6). The overall correlation of retreat to period with this combination of separation events is –0.99 (-0.96 with unedited point number 3). Why this may be physically plausible will be explored in the following discussion.

4. DISCUSSION

My overall goal in this study was to show that an objective Loop Current tracking technique could give eddy separation periods comparable to those determined by subjective tracking. This goal has been achieved. Furthermore, the objective technique provides a continuous time series of metrics for study of Loop Current intrusion and eddy separation. The time series presented, their statistics and the identified separation events, which have been validated by comparison with other observations, are the primary results of the successful implementation of this method. Although the Loop Current separation is not a well-defined discrete event, using the breaking of the tracking contour works remarkably well. The

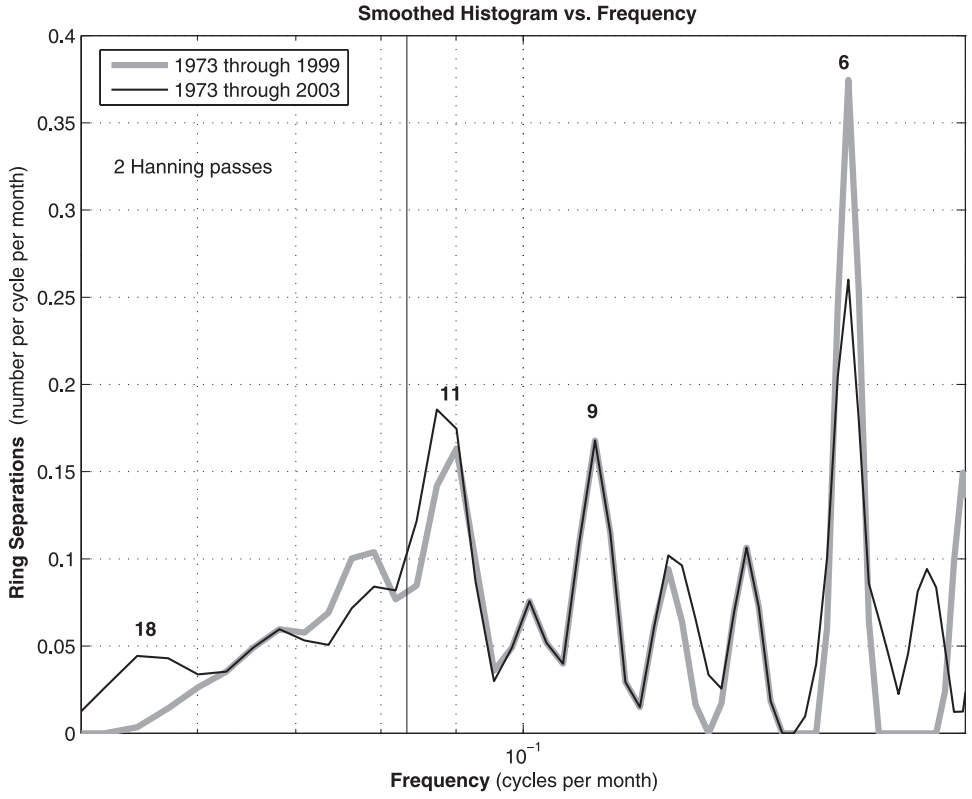

Figure 3. Smoothed histograms of Loop Current ring separation periods plotted to resemble a variance-preserving spectra after Sturges (1994) calculated from 1973-1999 events [*Sturges and Leben*, 2000] and 1973-2003 events including the objective separation estimates from the altimeter record (1993-2003) as described in this paper. The distributions have been smoothed by two Hanning passes. Values at intervals shorter than 5 months and longer than 20 months are off the scale. The vertical solid line is the annual frequency.

objective estimates fall within the subjective error estimates for separation events from the same time period reported in *Sturges and Leben* [2000]. Given that nonsystematic errors in separation time do not cancel when calculating the separation period, more work still needs to be done to estimate the uncertainty in the separation period determined by the objective tracking technique. For example, the 17-cm contour may break at different times or stages within the continuous separation process for the wide variety of events that have been observed. Using several tracking contours and looking at the spread of the estimated separation times may be one way to quantify this error.

The fundamental result of the spectral analyses performed on the objective tracking analyses for this study is that the Loop Current exhibits significant power near 6, 9, and 11 months, and little or no power exactly at the annual frequency in agreement with the results presented in *Sturges and Leben* [2000]. These are robust results that are exhibited by the histogram, smoothed histogram and FFT spectra analyses.

The conspicuous absence of annual power merits further discussion. It has been speculated that the lack of power at 12 months is caused by a beat-frequency effect [*Sturges,* 1992; *Sturges and Leben*, 2000]. The premise is that the power at a lower frequency modulates the power at the annual period, giving rise to the observed spectral peak. The standard relationship between frequencies is:

$$f_1 \pm f_2 = f_3$$

where f_1 is annual, f_2, is the unknown, and f_3 is the peak observed near 11 months. The unknown values vary from 132 to 276 months for the corresponding 11- to 11.5- month peaks seen in the smoothed histogram and FFT spectra (Figures 3 and 4).

Unfortunately, these values are beyond the resolution of the 11.5-year (138-month) time series of altimeter observations used to calculate the FFT spectrum and cannot be studied using the histogram technique from the longer time series of separation periods. The lowest frequency observed in the FFT spectrum (Figure 4) is near 67 months, which is

approximately half of the decadal time scale associated with climate signals over the North Atlantic and may be a harmonic of the decadal signal yet to be observed using a longer data record. A much longer record is needed to resolve the power associated with the 11- and 12-month signals. Using a conservative estimate of two times the Raleigh criterion [*Emery and Thompson*, 1998], a 22- to 46-year-long times series would be required to resolve the annual signal from 11- to 11.5-month peaks, respectively.

One caveat concerning the objective Loop Current tracking and annual signals is that the altimetric analysis uses along-track data that has been high-pass filtered. This processing may remove the basin-scale steric signal associated with surface heating and cooling that can be as large as 5 to 8 cm in the Gulf [this estimate is based on unfiltered T/P and Jason over the Gulf] and exhibit power at the annual frequency. This signal, however, would be present in model simulations incorporating realistic heat fluxes. The overall effect on separation periods should be minimal, but some additional power may be present in FFT spectra from model data that is not present in the altimetric analysis.

Another conclusion of this study is that the altimeter-derived estimates of Loop Current metric statistics are in very good agreement with earlier studies based on in situ and radiometry observations. These earlier studies span time periods comparable to the altimetric record with little or no overlap in time and support the conjecture that the fundamental Loop Current behavior is nearly stationary. The agreement of mean and standard deviations and the implied stationarity is not surprising considering the topographic confinement of the current and the fundamental physical control of the dominant eddy-shedding cycle. The distributions of the individual Loop Current metrics shown in the histograms included in Plates 1 and 2, however, are clearly non-Gaussian. Although the mean and standard deviation of the metric time series are stable over different time periods, even in the presence of the irregular eddy separation cycle it is unlikely that the overall distributions are stationary because of the strong influence of the irregular eddy separation cycle and the limited number of total events observed. This effect is seen in the separation period histograms for the time periods of 1973-1992 and 1993-2003 shown in the lower panels of Figure 2. One might argue that the differences in the distributions are an artifact of the techniques and data coverage used to identify eddy separation and estimate the separation period. A counterpoint to this argument is that the

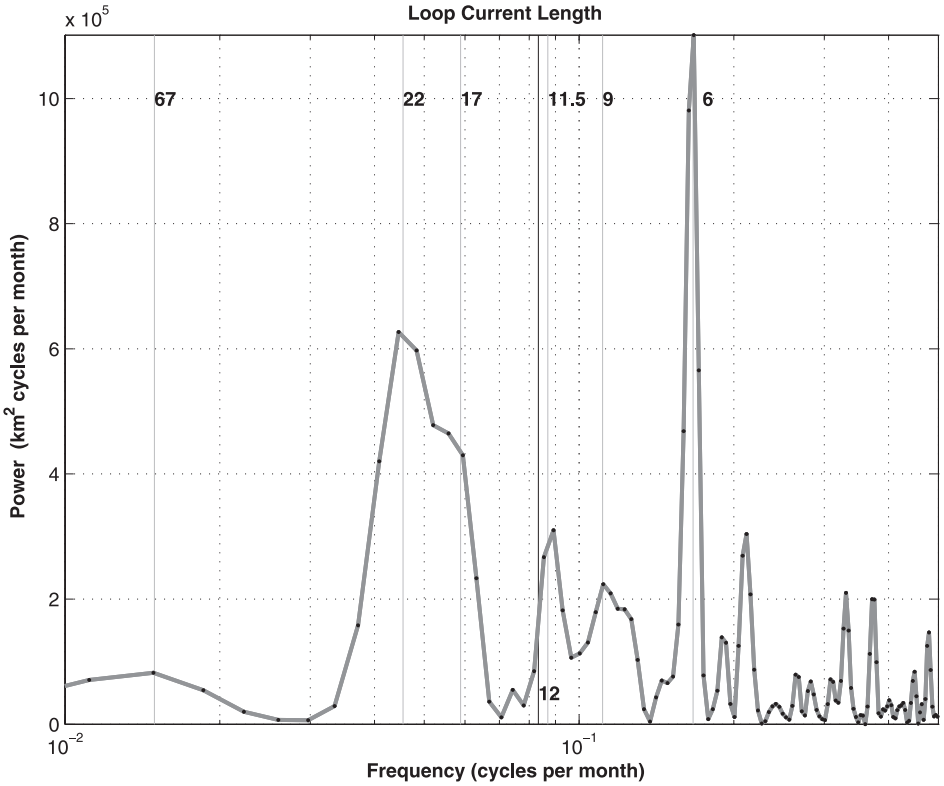

Figure 4. FFT power spectrum of the Loop Current length estimated from the daily 1/1/1993 through 7/1/2004 altimeter-derived time series. The light gray lines highlight periods (in months) associated with selected frequencies.

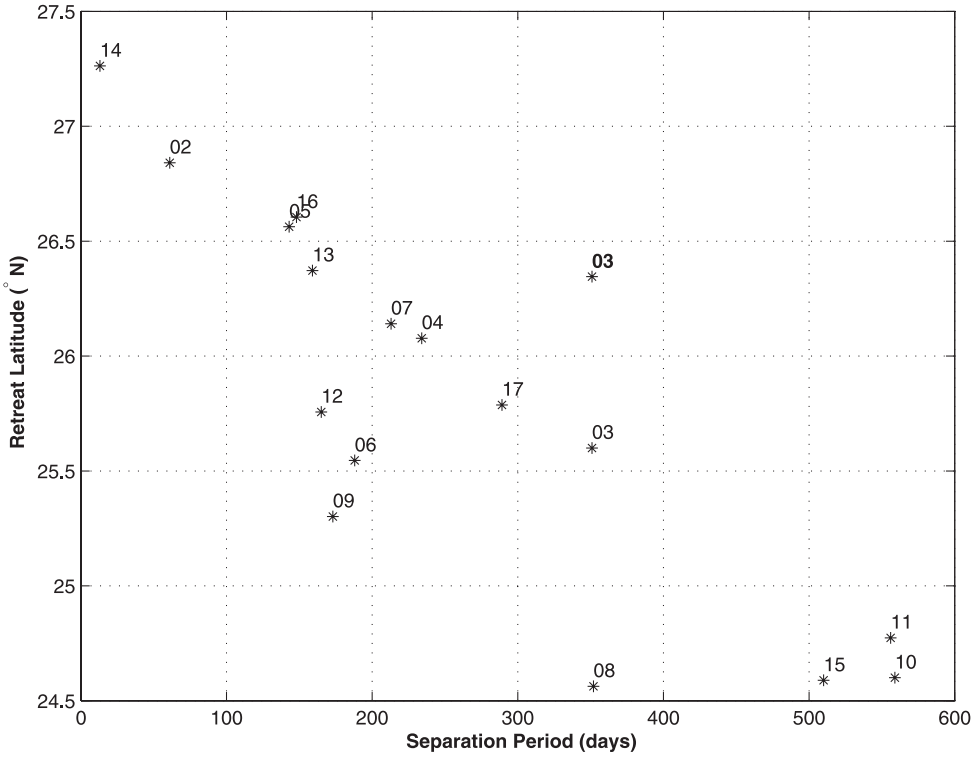

Figure 5. Plot of separation period versus the retreat latitude of the Loop Current immediately following the previous eddy separation. The points are numbered according to the events shown in Plate 4. See text for discussion of the repeated point number 3.

Gulf was reasonably well observed in the 1980s and early 1990s, and if the eddy separations were counted in a similar manner, then the distributions are quite different. In comparison to the earlier record, there are clearly more 18-month separation periods and fewer 12- to 16-month separation periods observed in the altimeter record.

The relationship between Loop Current retreat and subsequent eddy separation periods is a new result (Figure 5) and may be the first significant prognostic or leading indicator for predicting a Loop Current metric statistically. Several other physical quantities have shown correlation with Loop Current intrusion, which are diagnostic in nature in that they identify a coincident process in correlation with the Loop Current variability. Some examples are the deep outflow through the Yucatan channel [*Bunge et al.*, 2002, *Ezer et al*., 2003] and the integrated vorticity influx [*Candela et al*., 2002].

The correlation between Loop Current retreat and subsequent eddy shedding is interesting because it contradicts a basic assumption of the theory of *Pichevan and Nof* [1997]. This has led to a strawman hypothesis that the timing of the Loop Current penetration and separation is affected more by the initial condition of the Loop at the onset of reintrusion than by the various dynamical mechanisms that interact during intrusion to cause ring detachment. In a rough analogy to the analytic theory of *Pichevan and Nof* [1997], which predicts a periodic eddy separation cycle assuming the Loop Current returns to the same initial state after separation, a more realistic theory may be that an aperiodic (and maybe predictable) eddy cycle occurs because the Loop Current returns to different, seemingly random, initial states after each separation event. It is not clear that an analytical theory could be developed which accommodates the assumption that the Loop Current does not return to the same initial state. Note that the initial states need not be uniformly random. If the prior Loop Current retreat is well correlated with separation period, then the histogram of retreat latitudes will have peaks corresponding to the dominant periods in the histogram of separation period.

This leads to the question: What physical processes might set the initial state of the Loop Current after eddy separation? The short answer is: any processes that affect the amount of Loop Current water mass entrained into the separating eddy. These are the same processes that are implicated in eddy separation, such as those discussed in the introductory literature review in this paper. A leading candidate mecha-

nism is the interaction of the Loop Current with peripheral cyclones produced by instability modes and interactions with topography (see the paper in this volume by *Schmitz*). In terms of the retreat, the complicated interaction of anticyclonic and cyclonic eddies within the confines of the eastern deep Gulf basin determines the size of the separating eddy and thereby the initial state of the Loop Current after the separation event. Such vortex interactions and instabilities are highly nonlinear, and may explain the seemingly random nature of Loop Current eddy separation. Other processes, such as climate forcing, upstream conditions, momentum and vorticity fluxes may also play a role.

More controversial, in my opinion, is the nearly perfect linear relationship between retreat and period when eddy separation periods are combined in the manner described, which gives the impressive correlation shown in Figure 6. If this judicious combination of selected separation periods negates the influence of another physical mechanism or mechanisms that temporarily overrides the more fundamental physical relationship between retreat and shedding, then a remarkably fundamental physical property of the Loop Current has been discovered. Of course this begs the question, which in formal logic means that I have improperly assumed as true the very point I am trying to make. Nevertheless, for retreats above 26ºN, the linear relationship is quite robust. Below 26ºN other mechanisms and/or causes may be important. The easiest explanation is the miscounting of separation events, which is likely the case for Eddy 12, a marginal filament eddy that may not be associated with the dominant dynamics of Loop Current intrusion. Events 6 and 8, however, are energetic separation events that occur within the cycle of the "predicted" period. The separation of Eddy 6 involved a very strong companion cyclone to the east that remained in the area north of the Loop Current during the next event, arresting reintrusion and causing multiple detachments and reattachments of Eddy 7 before separation. Event 8, in contrast, appears to be a canonical eddy separation event at the dominant 11.5-month eddy separation period. Comparing the time series for Events 8 and 9, 10, 11 and 15 shows how irregular the character of the Loop Current can be in the time interval between initial retreat and separation for these deep southern retreat events. It is, therefore, not unrealistic to assume that large enough perturbations to the system could occur that would impact the "predicted" aperiodic behavior of the Loop Current and occur at one of the dominant frequencies of the dynamical system. Of course, without a more complete understanding of the dynamics involved in Loop Current intrusion, separation and retreat, this may just be a statistical artifact leading to physically implausible speculation.

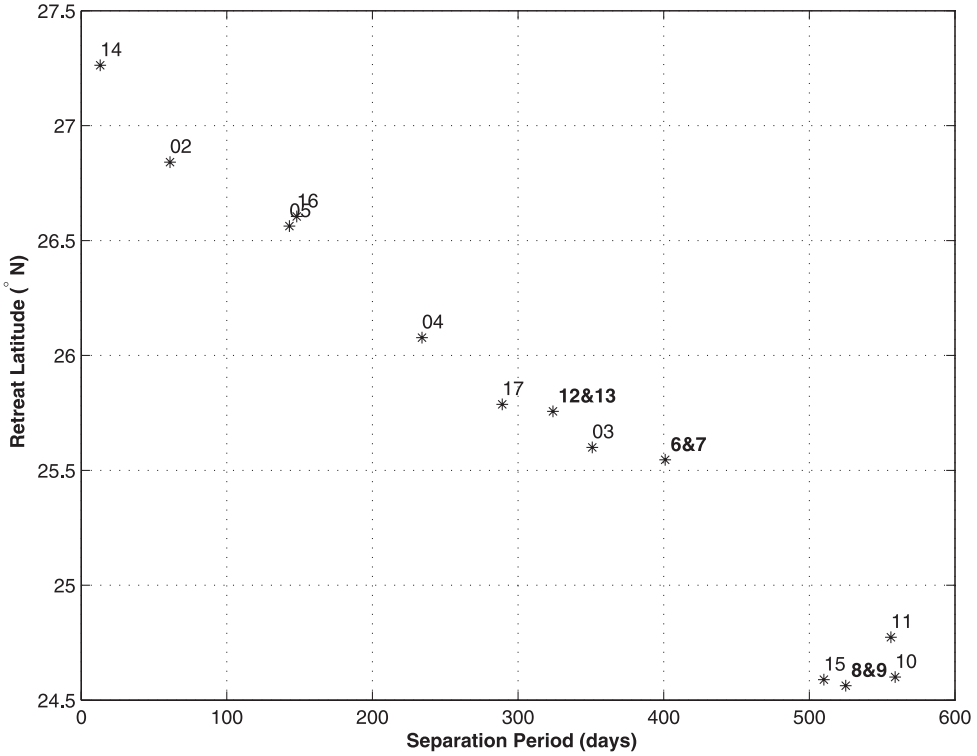

Figure 6. Same as Figure 9, but with selected sequential separation events combined.

If the linear relationship holds, then one could conclude that we have observed nearly the full dynamic range of Loop Current separation periods, which I estimate to be about zero (simultaneous separation of two Loop Current eddies) to 22 months. The upper bound is based on the period determined by a port-to-port retreat of the Loop Current, in which the entire current retreats below 24ºN immediately following a separation event. This is a realistic latitude for the southernmost retreat possible.

In conclusion, my discussion has been intentionally speculative to motivate future investigations of Loop Current dynamics through the careful analysis of the available observations. I specifically selected the Loop Current length for monitoring Loop Current separation primarily because it is a relatively easy metric to estimate from numerical model simulations. This is to encourage more quantitative comparisons of observations to model experiments. The comprehensive set of Loop Current metrics in this paper and the SSH animation included on the companion CD-ROM are intended to assist in these efforts.

Acknowledgements. I thank Kevin Corcoran for his help calculating the Loop Current metrics and plotting figures, Peter Gimeno for helping with data processing, and Dr. Chad Fox for collaborating with me to develop the MATLAB® Loop Current metric toolbox. Dr. Kenneth S. Casey kindly provided the SST data used in this study. Tony Sturges' insightful suggestions and comments contributed substantially to this work. The U.S. Minerals Management Service (MMS 1435-01-02-CT-31152; MMS 1435-01-04-CA-32645), the National Science Foundation (OCE-324688) and NASA (contract 1221120) provided funding for this study. I greatly appreciate their support.

REFERENCES

Abascal, A. J., J. Sheinbaum, J. Candela, J. Ochoa, and A. Badan (2003), Analysis of flow variability in the Yucatan Channel, *J. Geophys. Res.,* 108, No. 12, 3381, doi:10.1029/2003JC001922.

Berger, T. (1993), Loop Current eddy shedding cycle. *LATEX Program Newsleter*, Vol. 2, No. 24, College of Geosciences, Texas A&M University. [Available from Dept. of Oceanography, Texas A&M University, College Station, TX 77843–3146.]

Berger, T. J., P. Hamilton, J. J. Singer, R. R. Leben, G. H. Born and C. A. Fox (1996), Louisiana/Texas Shelf Physical Oceanography Program Eddy Circulation Study: Final Synthesis Report. Volume I: Technical Report, OCS Study MMS 96-0051, U.S. Dept. of the Interior, Minerals Management Service, Gulf of Mexico OCS Region, New Orleans, LA. 324 pp.

Bunge, L., J. Ochoa, A. Badan, J. Candela, and J. Sheinbaum (2002), Deep flows in the Yucatan Channel and their relation to changes in the Loop Current extension, *J. Geophys. Res.,* 107, 3223, doi:10.1029/2001JC001256.

Casey, K. S, and P. Cornilon (1999), A comparison of satellite and in situ based sea surface temperature climatologies, *J. of Climate*, Vol. 12, No. 6, 1848–1863.

Candela, J., J. Sheinbaum, J. Ochoa, A. Badan and R. Leben (2002), The potential vorticity flux through the Yucatan Channel and the Loop Current in the Gulf of Mexico, *Geophys. Res. Lett.,* 29, No. 22, 2059, doi:10.1029/2002GL015587.

Chérubim, L. M., W. Sturges and E. P. Chassignet (2004), Deep flow variability in the vicinity of the Yucatan Straits from a high-resolution numerical simulation, *J. Geophys. Res.,* 110, C04009, doi:10.1029/2004JC002280.

Cressman, G. P. (1959), An operational objective analysis system, *Mon. Weather Rev.*, 87, 367–374.

Emery, W. J., and R. E. Thompson (1998), *Data Analysis Methods in Physical Oceanography*, 634 pp, Pergamon, Tarrytown, N.Y.

Ezar, T., L. –Y. Oey, H.-C Lee, and W. Sturges (2003), The variability of currents in the Yucatan Channel: Analysis of results from a numerical ocean model, *J. Geophys. Res.*, 108(C1), 3012, doi:1029/2002JC001509.

Fratantoni, P. S., T. N. Lee, G. Podesta, and F. Muller-Karger (1998), The influence of Loop Current perturbations on the formation and evolution of Tortugas eddies in the southern Stratis of Florida, *J. Geophys. Res.,* 103, 24,759–24,779.

Hamilton P., Berger, T.J., J.H. Churchill, R.R. Leben, T.N. Lee, J.J. Singer, W. Sturges, and E. Waddell (2000), Desoto Canyon Eddy Intrusion Study; Final Report, Volume II: Technical Report, OCS Study MMS 2000-080, U.S. Dept. of Interior, Minerals Management Service, Gulf of Mexico OCS Region, New Orleans, LA. 269 pp.

Hurlburt, H. E., and J. D. Thompson (1980), A numerical study of Loop Current intrusions and eddy shedding, *J. Phys. Oceanogr.*, 10, 1611–1651.

Koblinsky et al. (1999), NASA Ocean Altimeter Pathfinder Project, Report 1: Data Processing Handbook, NASA/TM-1998-208605.

Leben, R. R., and G. H. Born (1993), Tracking Loop Current eddies with satellite altimetry, *Adv. Space. Res.*, 13, 325–333.

Leben, R. R., G. H. Born and B. R. Engebreth (2002), Operational altimeter data processing for mesoscale monitoring, *Marine Geodesy*, 25, 3–18.

Lee, T. N., K. Leaman, E. Williams, T. Berger and L. Atkinson (1995), Florida Current meanders and gyre formation in the southern Straits of Florida, *J. Geophys. Res.,* 100, 8607–8620.

Maul, G. A., and F. M. Vukovich (1993), The relationship between variations in the Gulf of Mexico Loop Current and Straits of Florida volume transport, *J. Phys. Oceanogr.* 23, 785–796.

Murphy, S. J., H. E. Hurlburt, J. J. O'Brien (1999), The connectivity of eddy variability in the Caribbean Sea, the Gulf of Mexico and the Atlantic Ocean, *J. Geophys. Res.,* 104, 1431–1453.

Nowlin, W. D., Jr., A. E. Jochens, S. F. DiMarco, R. O. Reid, and M. K. Howard (2001), Deepwater Physical Oceanography Reanalysis and Synthesis of Historical Data: Synthesis Report, OCS Study MMS 2001-064, U.S. Dept. of the Interior, Minerals Management Service, Gulf of Mexico OCS Region, New Orleans, LA. 530 pp.

Oey, L.-Y., H.-C. Lee and W. J. Schmitz (2003), Effects of winds and Caribbean eddies on the frequency of Loop Current eddy shedding: A numerical modeling study, *J. Geophys. Res.,* 108, 3324, doi:10.1029/20002JC001698.

Ohlmann, J. C., P. P. Niiler, C. A. Fox, and R. R. Leben (2001), Eddy energy and shelf interactions in the Gulf of Mexico, *J. Geophys. Res.,* 106, 2605–2620.

Pichevin, T. and D. Nof (1997), The momentum imbalance paradox, *Tellus,* 49A, 298–319.

Tierney, C. C., M. E. Parke, and G. H. Born (1998), An investigation of ocean tides derived from along-track altimetry, *J. Geophys. Res.*, 103, 10,273–10.287.

SAIC (1989), Gulf of Mexico Physical Oceanography Program, *Final Report: Year 5. Volume II: Technical Report*, OCS report/MMS-89-0068, U. S. Department of the interior, Minerals Management Service, Gulf of Mexico OCS Regional Office, New Orleans, LA. 333 pp.

Sturges, W. (1992), The spectrum of Loop Current variability from gappy data, *J. Phys. Oceanogr.*, 22, 1245–1256.
Sturges, W. (1994), The frequency of ring separations from the Loop Current, *J. Geophys. Oceanogr.*, 24, 1647–1651.
Sturges, W. and R. Leben (2000), Frequency of ring separations from the Loop Current in the Gulf of Mexico: A revised estimate, *J. Phys. Oceanogr.*, 30, 1814–1819.
Vukovich, F. M. (1988), Loop Current boundary variations. *J. Geophys. Res.,* 93, 15,585–15,591.
Vukovich, F. M. (1995), An updated evaluation of the Loop Current's eddy shedding frequency, *J. Geophys. Res.*, 100, 8655–8659.
Vukovich, F. M., and G. A. Maul (1985), Cyclonic eddies in the eastern Gulf of Mexico, *J. Phys. Oceanogr.*, 15, 105–117.
Wang, Y. M. (2001), GSFC00 mean sea surface, gravity anomaly and vertical gravity gradient from satellite altimeter data, *J. Geophys. Res.*, 106, 31167–31174.
Welsh S. U., and M. Inoue (2000), Loop Current rings and the deep circulation in the Gulf of Mexico. *J. Geophys. Res.*, 105, 16,951–16,959.
Zavala-Hidalgo, J., S. L. Morey and J. J. O'Brien (2003), Cyclonic eddies northeast of the Campeche Bank from altimetry data, *J. Phys. Oceanog.*, 33, 623–629.

Robert R. Leben, 431 UCB, Boulder, CO 80309-0431 (leben@colorado.edu)